Prepared for submission to JCAP HIP-2015-20/TH

Lattice Calculation of the Decay of Primordial Higgs Condensate

Kari Enqvist,[a] **Sami Nurmi,**[a,b] **Stanislav Rusak,**[a] **and David J. Weir**[c]

[a]University of Helsinki and Helsinki Institute of Physics, P.O. Box 64, FI-00014, Helsinki, Finland

[b]Department of Physics, University of Jyväskylä, P.O. Box 35 (YFL), FI-40014 University of Jyväskylä, Finland

[c]Faculty of Science and Technology, University of Stavanger, 4036 Stavanger, Norway

E-mail: kari.enqvist@helsinki.fi, sami.nurmi@helsinki.fi, stanislav.rusak@helsinki.fi, david.weir@uis.no

Abstract. We study the resonant decay of the primordial Standard Model Higgs condensate after inflation into SU(2) gauge bosons on the lattice. We find that the non-Abelian interactions between the gauge bosons quickly extend the momentum distribution towards high values, efficiently destroying the condensate after the onset of backreaction. For the inflationary scale $H = 10^8$ GeV, we find that 90% of the Higgs condensate has decayed after $n \sim 10$ oscillation cycles. This differs significantly from the Abelian case where, given the same coupling strengths, most of the condensate would persist after the resonance.

Contents

1 Introduction

After the detection of Standard Model (SM) Higgs [1, 2] there has been a growing interest in the cosmological role of the Higgs field Φ. Intriguingly, the Higgs might even act as the inflaton if its potential at high energies is dominated by a coupling to the spacetime curvature of the form $\xi\Phi^\dagger\Phi R$ [3]. The connection to the low energy SM regime of the scenario is, however, not unique due to its non-renormalizability [4–6] and the required large coupling $\xi \gtrsim 10^3$ could be subject to questions of naturalness [7–9].

However, the Higgs could also be of cosmological interest in several other ways. If the Higgs potential remains close to the SM form up to the inflationary scale H_*, during inflation the Higgs would be a light spectator field, as discussed in [10–17]. In such a case inflation needs to be driven by some new physics beyond SM. Like for all light fields during inflation, both the Higgs mean field as well as the local field value will be subject to fluctuations. The latter are isocurvature perturbations during inflation while fluctuations of the mean field generate an effective Higgs condensate. The condensate survives inflation and sets specific non-vacuum initial conditions for the hot Big Bang epoch [10, 12]. The typical magnitude of the Higgs mean field is, provided inflation lasts long enough, of the order of H_*. Depending on details of physics beyond SM the primordial Higgs condensate could have significant observational impacts ranging from imprints in CMB to baryogenesis and dark matter [11, 18–21].

Theoretical self-consistency of the setup requires a stable vacuum. As is well known, the pure SM vacuum in flat space becomes unstable above energies $\mu_c \sim 10^{10}$ GeV for the measured best fit values of the strong coupling constant, the top mass, and the Higgs mass $M_h \simeq 125$ GeV [10, 14–17, 22–26]. However, as discussed in [10, 27], during inflation the stability depends crucially also on the Higgs-curvature coupling $\xi\Phi^\dagger\Phi R$. This coupling is necessarily generated by radiative corrections even if ξ would be set to zero at some scale. A one-loop investigation [27] shows that vacuum stability can be maintained even within the

SM up to the maximal inflationary scale $H_* \lesssim 10^{14}$ GeV consistent with the tensor bound [28, 29], provided that $\xi_{\rm EW} \gtrsim 0.1$ at the electroweak scale.

Thus quite generically, immediately after inflation the Universe features a primordial Higgs condensate. In the case of Higgs inflation, in which the Higgs itself sets the dynamics, the Universe is dominated by the Higgs condensate, and its decay time directly determines the reheating temperature [30, 31]. On the other hand, within the SM, and in a broad class of its extensions, the condensate contributes very little to the energy density of the Universe. At the onset of hot Big Bang its large displacement from the SM vacuum could nevertheless have important ramifications for the subsequent evolution of the Universe [11, 18, 20, 21]. Thus even if the Higgs were a mere spectator during inflation, it can affect post-inflationary physics until the condensate eventually decays. In both cases a detailed understanding of the Higgs condensate decay is crucial in order to properly address the observational imprints.

At zero temperature the dominant decay channel for both the SM Higgs and the non-minimally coupled Higgs inflaton is the non-perturbative production of gauge bosons through a parametric resonance [12, 30–33]. The investigation of the resonance is complicated by the non-Abelian dynamics of the gauge field which have not been carefully explored so far. In the regime of broad resonance, realized for SM running of the gauge couplings, the non-Abelian terms are small during the first stages of the resonance but rapidly grow important as the exponential production of gauge fields starts to backreact on the dynamics of the Higgs condensate. The efficiency and duration of the resonant Higgs decay therefore cannot be reliably estimated without properly accounting for the non-Abelian couplings. In the limit of a narrow resonance, which could occur in specific extensions of the SM, the non-Abelian features affect the resonance dynamics already before the dynamical backreaction of gauge fields [32].

In this work we investigate the resonant decay of the Higgs into gauge bosons using numerical lattice simulations and accounting for the full non-Abelian dynamics. In particular, we compute the decay time of the subdominant SM Higgs condensate generated during inflation.

The paper is organized as follows. In Section 2 we present the framework to investigate the resonant Higgs decay and make some analytical estimates. In Section 3 we present the results of our full lattice computation of the Higgs decay which constitutes the main part of the paper. Finally we conclude in Section 4.

2 Resonant Higgs decay in Standard Model

During and shortly after inflation the energies are significantly higher than the electroweak scale. Thus the Standard Model Higgs potential can be approximated by the quartic term alone. The relevant part of the SM action for our discussion is

$$S = -\int \mathrm{d}^4x \left\{ \frac{1}{4}\eta^{\mu\alpha}\eta^{\nu\beta}\left(F^a_{\mu\nu}F^a_{\alpha\beta} + G_{\mu\nu}G_{\alpha\beta}\right) + a^4\left[(D_\mu\Phi)^\dagger D^\mu\Phi + \lambda(\Phi^\dagger\Phi)(\Phi^\dagger\Phi)^2\right]\right\} \tag{2.1}$$

with the kinetic terms

$$\begin{aligned} F^a_{\mu\nu} &= \nabla_\mu A^a_\nu - \nabla_\nu A^a_\mu + g\epsilon^{abc}A^b_\mu A^c_\nu \,, \\ G_{\mu\nu} &= \nabla_\mu B_\nu - \nabla_\nu B_\mu \,, \\ D_\mu\Phi &= \left(\nabla_\mu - igA^a_\mu\tau^a - \frac{i}{2}g'B_\mu\right)\Phi \,. \end{aligned} \tag{2.2}$$

Here Φ is the Higgs doublet and A^a_μ and B_μ are the SU(2) and U(1) gauge fields, respectively.

We assume that the inflationary stage is driven by some physics beyond the SM. To reheat the universe, the inflaton field, or fields, should arguably be coupled to the SM degrees of freedom through non-gravitational interactions. We assume these couplings are small and use the pure SM running for the Higgs and gauge couplings. More importantly, we will be investigating the decay of the Higgs field assuming there is no thermal background. If the inflaton has already decayed at this stage, we are therefore implicitly assuming that the interaction rate between its decay products and the SM fields is small compared to the Hubble time over our epoch of interest. On the other hand, one could argue that the decay rate of the inflaton field would typically be much smaller than the decay rate of the Higgs condensate. In such a case the oscillating inflaton field would give rise to an effectively matter dominated universe.

2.1 Initial conditions from inflation

Given the SM potential, the SM Higgs is both a light field and energetically subdominant during inflation [11, 12]. Its super-horizon dynamics can be investigated using the stochastic formalism [34, 35]. Starting from a generic field configuration at some point during inflation, the Higgs distribution relaxes to the equilibrium given by $P(h) \sim \exp(-8\pi^2 V/3H^4)$ within a time scale of $N_{\rm rel.} \simeq 100$ e-folds [36]. Provided that inflation lasted somewhat longer we can therefore quite generally assume that the value of the Higgs condensate in the observable universe is to be drawn from the equilibrium distribution.

After the end of inflation the typical mean Higgs field value over the observable universe is thus given by

$$h_* = \sqrt{\langle h^2 \rangle} = 0.36 \lambda_*^{-1/4} H_* \ . \tag{2.3}$$

The inflationary stage thus generates a primordial Higgs condensate h_*, setting specific non-equilibrium initial conditions for the Hot Big Bang epoch. Here we are implicitly assuming a low inflationary scale $H_* \lesssim 10^9$ GeV such that the Higgs coupling to curvature scalar $\xi \Phi^\dagger \Phi R$ can be neglected [27].

2.2 Onset of the resonant Higgs decay

The Higgs condensate becomes effectively massive as $H^2_{\rm osc} = 3\lambda_* h_*^2$ and it starts to oscillate around the vacuum expectation value $h = 0$. In terms of the rescaled field $\chi = ah$ and conformal time $d\tau = a^{-1} dt$ the equation of motion reads

$$\ddot{\chi} + \lambda \chi^3 - \frac{\ddot{a}}{a}\chi = 0 \ . \tag{2.4}$$

The last term can in general be neglected. In a radiation dominated background it is identically zero and for matter domination it becomes negligible soon after the onset of Higgs oscillations. The expansion of space can therefore be scaled out from the dynamics and the problem essentially reduces to flat space.

The resonant production resulting from coherent oscillations of scalar fields has been extensively studied in the literature [37–40]. Neglecting self-interactions, the weak transverse components of the gauge fields obey the Lamé differential equation

$$\frac{\mathrm{d}^2 \mathbf{A}^T}{\mathrm{d}z^2} + \left[\kappa^2 + q\, \mathrm{cn}^2 \left(z, \frac{1}{\sqrt{2}} \right) \right] \mathbf{A}^T = 0. \tag{2.5}$$

where

$$z \equiv \sqrt{\lambda\chi_{\rm osc}^2}(\tau - \tau_{\rm osc}), \qquad \kappa^2 \equiv \frac{k^2}{\lambda\chi_{\rm osc}^2}, \qquad q \equiv \begin{cases} \frac{g^2}{4\lambda} & \text{for the W bosons} \\ \frac{g^2+g'^2}{4\lambda} & \text{for the Z boson} \end{cases}, \tag{2.6}$$

and q is the resonance parameter characterizing the strength of particle production. For the pure Standard Model this parameter is always greater than unity, which puts the system in the broad resonance regime [32]. The Lamé equation exhibits instability regions where the solutions are amplified exponentially resulting in explosive production of gauge boson quanta.

The exponential production of gauge fields could in principle be washed out by rapid perturbative decays of the generated gauge fields. This is indeed what happens in the early stages of reheating after the Higgs inflation [30, 31]. For the energetically subdominant SM Higgs this is however not the case. The perturbative decay rate of W bosons into any pair of fermions is small compared to the characteristic time scale of Higgs oscillations

$$\frac{\Gamma_W}{m_\chi} = \sqrt{3}32\pi\frac{g^3}{\sqrt{\lambda}} = \mathcal{O}(0.01)\ . \tag{2.7}$$

Similar estimates hold for the Z bosons. The perturbative decays are therefore irrelevant compared to the resonant production of gauge fields and can be neglected in what follows.

2.3 Backreaction and limitations of the analytical approach

In the discussion of the previous section we have ignored the non-Abelian interactions of the gauge fields as well as the backreaction of the produced particles on the dynamics of the Higgs field. This is justified in the beginning of the resonance where the gauge field occupation numbers are small.

As the occupation numbers grow larger than one, the non-Abelian terms backreaction effects eventually start to dominate the dynamics. Using the Hartree approximation one can estimate the onset of backreaction by evaluating the time when [32]

$$\frac{g^2}{2}\langle W_\mu^+ W^{\mu-}\rangle + \frac{g^2+g'^2}{4}\langle Z_\mu Z^\mu\rangle \sim 3\lambda\chi^2\ . \tag{2.8}$$

The backreaction destroys the coherence of the Higgs oscillations and eventually shuts down the resonance [38–40]. The dynamics in this regime is entirely dominated by interactions and its analysis requires a full non-linear lattice computation. Before turning to the numerical results in the next section let us however present some qualitative comments on the role of non-Abelian interactions.

For Abelian fields the distribution of occupation numbers would retain its form peaked around $\kappa \sim q^{1/4}/2$ and essentially a vacuum configuration for $\kappa \gg q^{1/4}$. The low energetic gauge bosons and Higgs particles $\kappa \lesssim q^{1/4}$ would be inefficient in fragmenting the remnants of the Higgs condensate. Consequently, it would seem that a significant part of the condensate would survive long after the backreaction.

The non-Abelian interactions of the W bosons however completely change the picture. As the occupation numbers around the resonant peak $\kappa \sim q^{1/4}/2$ grow much larger than unity the W scatterings and annihilations into Z bosons rapidly generate excitations with higher momenta. This generates a bath of gauge bosons extending to $\kappa \gg q^{1/4}$ which would appear to efficiently destroy the remnants of the Higgs condensate, in sharp contrast with

the Abelian case. As we will discuss below, this behaviour is exactly what we see in our numerical computation.

We should note here that also annihilations of the gauge bosons into two fermions participate in the Higgs decay. Indeed, the vacuum cross sections of the processes $WW \to f\bar{f}$ and $WW \to WW$ both scale as $\sigma \sim \alpha_W^2/m_W^2$ and the production of light fermions is also kinematically favoured, as discussed in the context of preheating after the Higgs inflation [30, 31]. However, at the final stages of the resonance the non-Abelian interactions $WW \to WW, WW \to Z$ are significantly favoured by the large occupation numbers $n_{W,Z} > 1$. In our lattice computation we will therefore neglect the decay channels into light fermions.

3 Full lattice computation of the Higgs decay

Motivated by the considerations above, we simulate the SM Higgs dynamics on lattice during the period over which exponential production of gauge bosons is taking place. As the Higgs decay proceed dominantly through the production of non-Abelian W bosons we simplify the problem by investigating a SU(2) gauge-Higgs system instead of the full SU(2) $\times$ U(1) symmetry. Technical details of the lattice simulation can be found in Appendix A. The techniques we use are similar to those employed in previous numerical studies of preheating involving gauge fields [41–43].

Note that the system under consideration is conformal and so the effect of expansion can be neglected. Therefore there is no mass scale, other than that set by the initial value of the Higgs field.

Our initial conditions for the gauge field are Gaussian white noise with strength ξ,

$$\langle A_i^a(k,0) A_j^b(k',0)\rangle = \xi \delta^{ab}\delta_{ij}\delta(k-k') \ . \tag{3.1}$$

rather than the quantum vacuum. To avoid needing to carry out projection to satisfy the Gauss law initially, we assume that the gauge field conjugate momentum is initially zero. The gauge field equilibrates quickly, in any case, and loses all memory of these initial conditions as the particle number starts to grow. We then take as $z = 0$ the time when the particle occupation number at the peak of the resonance exceeds $n_\kappa = 0.1$.

We have confirmed that the normalization ξ of the gauge field initial conditions only has a logarithmic impact on the time taken for the system to equilibrate. For the purposes of the current paper, then, the above Gaussian noise initial conditions are adequate.

The lattice simulations are carried out in temporal gauge, which is equivalent to setting $A_0 = 0$, however we must further fix lattice Coulomb gauge to recover particle numbers. When we wish to measure particle numbers in the gauge field we use standard gauge fixing techniques (see Appendix A.1) and then measure the connected two point functions [43–45]

$$\left\langle A_i^a(\mathbf{k},t) A_j^b(-\mathbf{k},t)\right\rangle = \delta_{ab}\left[\left(\delta_{ij} - \frac{k_i k_j}{k^2}\right) D_T^A(k,t) + \frac{k_i k_j}{k^2} D_L^A(k,t)\right], \tag{3.2}$$

$$\left\langle E_i^a(\mathbf{k},t) E_j^b(-\mathbf{k},t)\right\rangle = \delta_{ab}\left[\left(\delta_{ij} - \frac{k_i k_j}{k^2}\right) D_T^E(k,t) + \frac{k_i k_j}{k^2} D_L^E(k,t)\right]. \tag{3.3}$$

With $D_L^A(k,t) = 0$ in Coulomb gauge we define the gauge field particle number as

$$n_k^A(t) = \sqrt{D_T^A(k,t) D_T^E(k,t)}. \tag{3.4}$$

This quantity is not gauge invariant and so we also present the power spectrum of the energy density in the gauge field in our results. This observable does not show the clear sharp resonant peak but it does allow one to identify backreaction and the onset of equilibration.

For comparison we also plot the results of a 'non-compact' U(1) simulation with equivalent initial conditions[1]. A comprehensive numerical study of the resonant production of Abelian gauge bosons was recently carried out in Ref. [33], and so we will not go into detail here.

In general we use lattices of volume 128^3. With gauge fixing, each simulation at this volume typically required four hundred CPU-hours; in total the results of this paper required less than ten thousand CPU-hours. On the infrared side we varied the lattice volume to ensure that the parametric resonance was not unacceptably cut off at long wavelengths, and confirmed that the results of this paper do not depend on this. It is less straightforward to establish that the physics does not depend on rescaling the system, because it is conformal and there is no mass scale.

To provide a numerical estimate of the time taken for the Higgs field to backreact, we define the *backreaction time* $z_{\rm br}$ as the time when the amplitude of the Higgs oscillations falls to 90% of its initial value h_*. We emphasise, however, that this time is logarithmically dependent on the amplitude ξ of the initial conditions for the gauge field. The simulations presented here are however more than sufficient to demonstrate the correct qualitative behaviour.

After the backreaction on the Higgs commences, the system starts to equilibrate and the equation of state for the scalar field approaches the equipartition value (1/3). We also see indications of thermalisation. However, because we do not have a mass scale in our simulations, we cannot give a definitive estimation of the thermalisation time. This must be left to future work that fully incorporates expansion.

3.1 Results

To give a broad resonance peak within our lattice volume we rescaled the system so that the lattice spacing is unity and work with rescaled lattice Higgs field $\Phi = 2\chi$.

In Figure 1 we show how the backreaction time varies with q for the noise amplitude. For the Standard Model changes of $q = g^2/(4\lambda)$ correspond to changes of the inflationary scale H_* which determines the values of the running coupling constants, identifying the renormalization scale as $\mu = h_* \sim H_*$; see Eq. (2.3). For example, taking $H_* = 10^8$ GeV yields with the SM running and best fit inputs the coupling values $g \simeq 0.6$ and $\lambda = 0.15$ at the end of inflation [23]. This gives the resonance parameter $q = g^2/(4\lambda) \sim 6$. The peaks (slowest to backreact) are associated with the values of q where the first (lowest-momentum) resonant band encountered is farthest from $\kappa = 0$.

Figure 2 depicts the time-evolution of the non-Abelian gauge field particle numbers. For the sake of comparison, we have also shown the time evolution in an Abelian case with equivalent Higgs and gauge coupling strengths. The initial evolution is similar in both cases but a drastic difference is observed as the particle numbers become much larger than unity. After this point the non-Abelian distribution is rapidly extended towards higher momenta through mutual interactions of the gauge bosons. In the Abelian case, where the interactions

[1]Note that a lattice simulation of 'compact' U(1) would not correctly show the onset of backreaction as the photon field $A_i(x)$ would be symmetric under transformations $A_i(x) \to A_i(x) + 2n\pi$. For the same reason, it is not sufficient to only initialise one colour of the SU(2) gauge field to get an 'abelian' comparison to the nonabelian case.

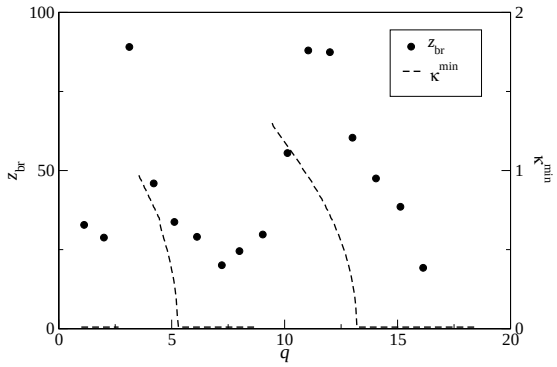

Figure 1: Plot of the backreaction time $z_{\rm br}$ against q for the non-Abelian theory. It seems that some fine tuning is required to substantially change the Higgs decay time. Also shown is the smallest κ that lies within a resonance band at a given q (for a full contour plot of resonance bands see e.g. Ref. [37]).

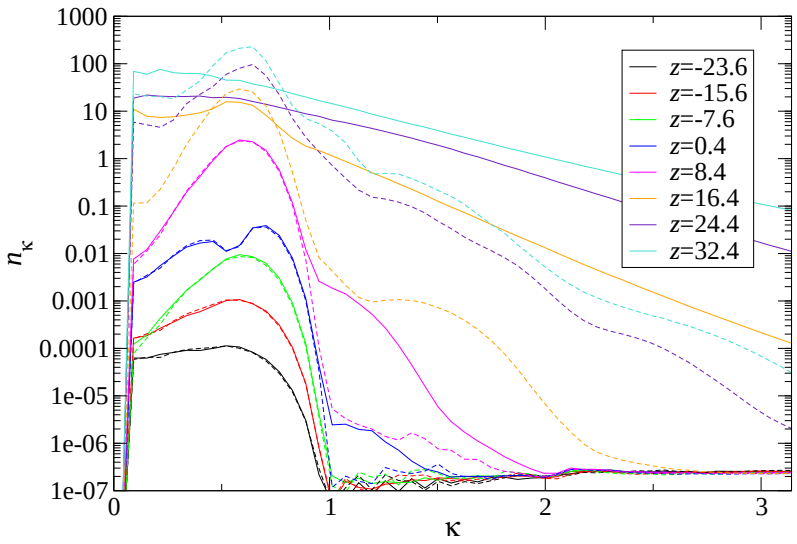

Figure 2: Comparison of particle numbers n_κ for abelian (dashed lines) and non-Abelian (solid lines) simulations ($q \approx 6.12$) evaluated at evenly-spaced time intervals. Equilibration in the abelian case is much slower and particle numbers remain many orders of magnitude smaller.

are absent the distribution on the other hand remains strongly peaked around the momenta $\kappa \lesssim q^{1/4}$ excited by the resonance. Similar behaviour can also be observed in the gauge field energy densities illustrated both for the Abelian and non-Abelian case in Figure 3

The bath of non-Abelian gauge particles with momenta extending to $\kappa \gg q^{1/4}$ rapidly destroys the Higgs condensate through scattering processes. This can be observed in Figure 4 which depicts the evolution of the various energy components of the Higgs and SU(2) gauge fields. Comparing Figures 2 and 4 we clearly see that the Higgs condensate rapidly starts

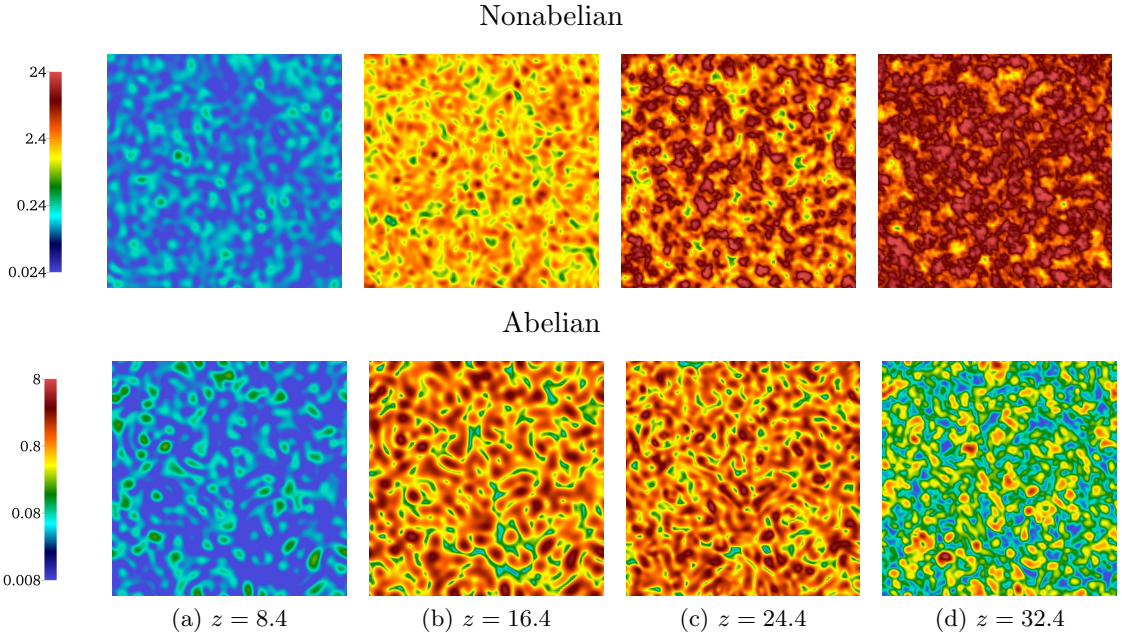

(a) $z = 8.4$ (b) $z = 16.4$ (c) $z = 24.4$ (d) $z = 32.4$

Figure 3: Slices of the gauge field energy density, comparison between Abelian and non-Abelian simulations, $q = 6.12$, at successive time-slices. Backreaction for the non-Abelian case has clearly started before $z \approx 24$ and the non-Abelian self-interaction means that by $z \approx 32$ the field configuration is no longer 'smooth'. In contrast, the Abelian simulation is still dominated by resonant structures at $z \approx 32$. The factor of three difference in the legend normalizations is due to the additional non-Abelian colour degrees of freedom.

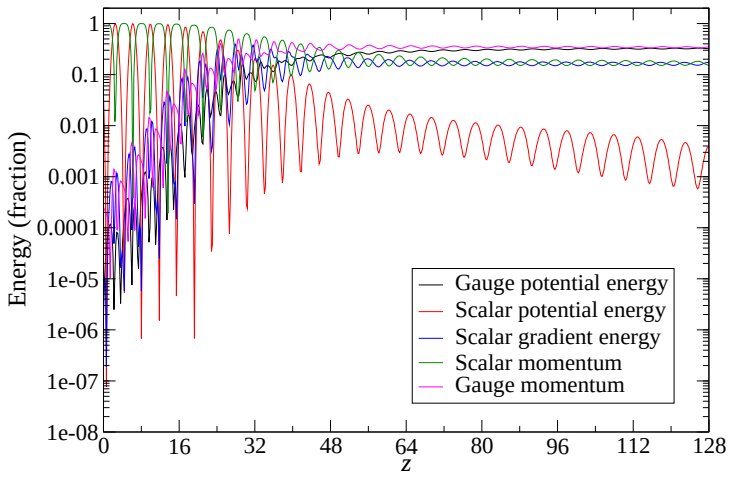

Figure 4: Time evolution of the individual energy components for a typical non-Abelian simulation ($q \approx 6.12$).

to decay after the gauge boson particle numbers at the resonance peak have ceased their exponential growth. The resonance shuts off and the remnants of the Higgs condensate decay completely within a few oscillation cycles.

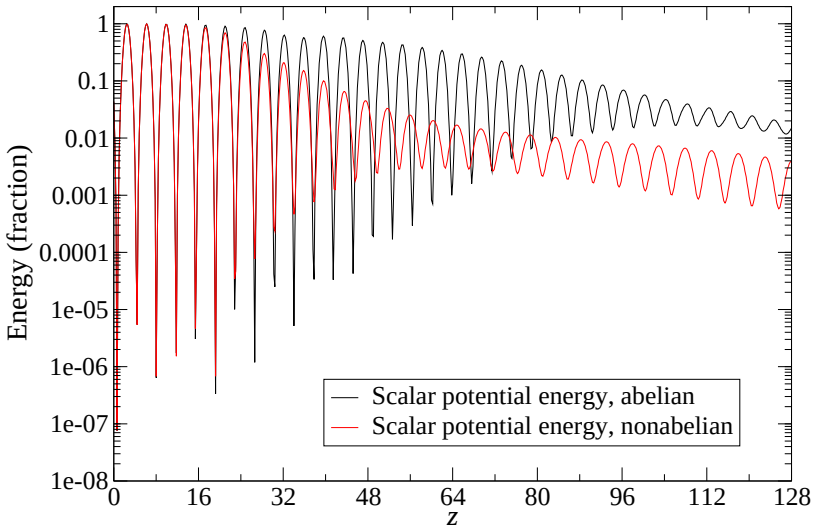

Figure 5: Comparison of scalar potential energies for Abelian and non-Abelian simulations ($q \approx 6.12$). The decay of the Higgs condensate is substantially faster in the non-Abelian case.

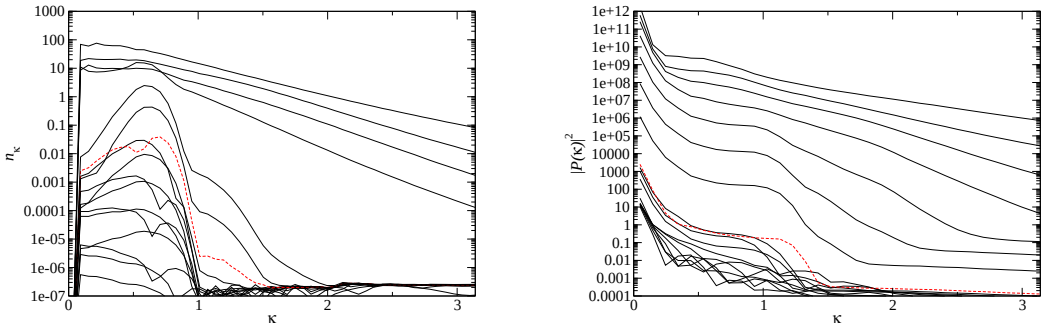

Figure 6: Plots showing (at left) the particle numbers n_κ and (at right) the power spectrum of the non-Abelian gauge field, at equal times (intervals of $\delta z = 4$) throughout a typical simulation ($q \approx 6.12$). The power spectrum closest to $z = 0$, at $z = 0.4$ is shown in both plots as a red dashed line.

In the Abelian case, a significant fraction $\mathcal{O}(1)$ of the condensate remains even after the end of resonance. This is illustrated in Figure 5 where we compare the evolution of the condensate energy in the Abelian and non-Abelian case. As discussed above, in the Abelian case the gauge field distribution remains peaked around the long-wavelength modes $k \lesssim q^{1/4}$ excited by the resonance. Correspondingly, the gauge boson scatterings of the Higgs field are not sufficient to destroy the condensate and the Higgs remains close to its initial non-equilibrium configuration.

Finally, in Figure 6 we show the development of particle number for a non-Abelian simulation at finer time intervals than is possible in figure 2, as well as the gauge field power spectrum for the same intervals, to give a gauge-invariant picture of the energy deposited in the bosons.

Note that the results presented here (and in particular Figure 2) bear a strong resemblance to Figure 7 in Ref. [46]. The underlying physics of equilibration and, presumably, subsequent thermalisation is very similar. Corresponding results have also been obtained for tachyonic preheating in Ref. [43].

4 Conclusions

In this work we have studied the non-perturbative decay of the primordial Higgs condensate after inflation into SU(2) gauge bosons which are produced through parametric resonance once the condensate leaves slow-roll and starts to oscillate. We performed a full lattice simulation of the resonant production of gauge bosons focusing in particular on the detailed dynamics after the onset of backreaction and carefully accounting for the effects arising from non-Abelian interactions.

Resonant decay of the condensate results in the production of particles within particular bands of momenta in the infrared region. However, we have found that the scattering and decay processes resulting from non-Abelian interactions rapidly extend the momentum distribution into the ultraviolet, which efficiently destroys the remnants of the Higgs condensate after the onset of backreaction. This is in sharp contrast to the purely Abelian case where the distribution remains in the infrared for much longer and the produced particles do not efficiently destroy the condensate so that a sizeable part of it survives after the resonance is terminated.

The time for backreaction to set in and the Higgs condensate to decay is found to be logarithmically dependent on the inflationary scale H_* which determines the Higgs initial conditions. For $H_* = 10^8$ GeV we find that 90% of the Higgs condensate has decayed after $n \sim 10$ oscillation cycles.

After the decay is completed the system starts to evolve towards equilibrium. Energy is rapidly transferred from the initially occupied IR modes towards higher momenta and the system appears to evolve towards a stationary state. This resembles the self-similar behaviour observed in earlier lattice studies of preheating [47, 48] and also studies of heavy ion collisions, see e.g. [49, 50]. The evolution of this stage towards the full thermal equilibrium can however not be analysed within a classical simulation which fails in describing the UV modes. We leave a more detailed investigation of the thermalisation for a future work.

We have emphasized that unless the SM Higgs sector is significantly modified by new physics, a Higgs condensate is inevitably generated during inflation. Thus it is important to understand the details of its decay as it may be significant for subsequent physics. The Higgs condensate sets specific out-of-equilibrium initial conditions for the hot Big Bang epoch which could have significant ramifications ranging from primordial perturbations and baryogenesis to non-thermal production of dark matter [11, 18–21]. In all these cases the decay time of the Higgs condensate is a crucial factor affecting the observational impacts. Our results indicate that, in the absence of thermal bath, once the Higgs condensate unfreezes and starts to oscillate it decays completely after $\mathcal{O}(10)$ oscillation cycles.

While we have considered the decay of the condensate within the context of the Standard Model it would be interesting to extend the analysis to the case of Higgs inflation, where the condensate plays the role of the inflaton through a large non-minimal coupling to gravity. While order of magnitude corrections to previous estimates [30, 31] are not expected, a proper inclusion of non-Abelian interactions appears crucial to precisely determine the predicted reheating temperature of the scenario. Other extensions of the Standard Model may also

be of interest. For instance, in some extensions the resonance might turn out to be narrow rather than broad. In such a case the non-Abelian nature of the interactions is expected to become important already before the onset of backreaction [32].

Acknowledgments

The numerical simulations were performed on the Norwegian computer cluster Abel, under the NOTUR project. SN is supported by the Academy of Finland grant 257532. SR is supported by the Magnus Ehrnrooth Foundation. DJW is supported by the People Programme (Marie Skłodowska-Curie actions) of the European Union Seventh Framework Programme (FP7/2007-2013) under grant agreement number PIEF-GA-2013-629425. We acknowledge useful discussions with Tommi Markkanen, Kari Rummukainen and Anders Tranberg.

A Details of lattice implementation

The lattice Hamiltonian is

$$H = \sum_x \pi^\dagger(x)\pi(x) + \sum_{x,i,a} \frac{1}{2} P_i^a(x) P_i^a(x) + \frac{2}{g^2} \sum_{x,i<j} \left[2 - \mathrm{Re}\,\mathrm{Tr}\, U_i(x) U_j(x+\hat{i}) U_i^\dagger(x+\hat{j}) U_j^\dagger(x) \right] + \sum_{x,i} \left[2\phi^\dagger(x)\phi(x) - 2\mathrm{Re}\,\phi^\dagger(x) U_i(x) \phi(x+\hat{i}) \right] + \sum_x V(\phi^\dagger(x)\phi(x)) \quad \text{(A.1)}$$

where π and P are the conjugate momenta for the Higgs and gauge fields, $U_i(x)$ are the link variables corresponding to the gauge field (see below) and ϕ is the Higgs field. The equations of motion are then

$$\phi(t+\delta t, x) = \phi(t,x) + \delta t\, \pi(t+\delta t/2, x) \quad \text{(A.2)}$$

$$U_i(t+\delta t, x) = \exp\left[-i \frac{g}{2} P_i^a(x, t+\delta t/2) \sigma^a\, \delta t \right] U_i(t,x) \quad \text{(A.3)}$$

$$\pi(t+\delta t/2, x) = \pi(t-\delta t/2, x) + \delta t \left[\sum_i \left[U_i(t,x)\phi(t,x+\hat{i}) - 2\phi(t,x) + U_i^\dagger(t,x-\hat{i})\phi(t,x-\hat{i}) \right] - \frac{\partial V}{\partial \phi^\dagger} \right] \quad \text{(A.4)}$$

$$P_k^m(t+\delta t/2, x) = P_k^m(t-\delta t/2, x) + \delta t \left[g\, \mathrm{Re} \left[\phi^\dagger(t, x+\hat{k}) U_k^\dagger(t,x) i\sigma^m \phi(t,x) \right] - \frac{1}{g} \sum_i \mathrm{Tr} \left[i\sigma^m U_k(t,x) U_i(t, x+\hat{k}) U_k^\dagger(t, x+\hat{i}) U_i^\dagger(t,x) + i\sigma^m U_k(t,x) U_i^\dagger(t, x+\hat{k}-\hat{i}) U_k^\dagger(t, x-\hat{i}) U_i(t, x-\hat{i}) \right] \right] \quad \text{(A.5)}$$

on the lattice, with Gauss law

$$G(x) = \sum_i \mathrm{Tr} \left[i\,\sigma^k P_i(t+\delta t/2, x) - i\,\sigma^k U_i^\dagger(t, x-\hat{i}) P_i(t+\delta t/2, x-\hat{i}) U_i(t, x-\hat{i}) \right] + 2g\, \mathrm{Re} \left[\pi^\dagger(t+\delta t/2, x) i\sigma^k \phi(t,x) \right] = 0. \quad \text{(A.6)}$$

See for example Refs. [41–43] for more details.

Our measurements of non-Abelian gauge boson particle number use a lattice approximation to $A_i^a(x,t)$. Given the parallel transporter is defined through

$$U_i(x,t) = \exp\left[-ig\frac{\sigma^a}{2}A_i^a(x+\hat{\imath}/2,t)\right] \tag{A.7}$$

we deduce

$$A_i^a(x,t) = \frac{i}{g}\mathrm{Tr}\,\sigma^a U_i(x,t) \tag{A.8}$$

to second order in the lattice spacing.

A.1 Gauge fixing in SU(2)

Our equations of motion are in temporal gauge, and so while at some point the system may be in Coulomb gauge, the time evolution of the system will generally take it away from this form. We fix Coulomb gauge on the lattice [51, 52], when we wish to measure particle numbers. To do this we must find a lattice gauge transformation $g(x) \in \mathrm{SU}(2)$ such that

$$F^g[U] = \frac{1}{6V}\sum_{x,i}\mathrm{Re}\,\mathrm{Tr}\,U_i^g(x) \tag{A.9}$$

is stationary, where

$$U_i^g(x) \equiv g(x)U_i(x)g^\dagger(x+\hat{\imath}). \tag{A.10}$$

We look for a maximum of this expression by carrying out a combination of simulated annealing and overrelaxation steps, a strategy that is widely used for lattice quantum field theory simulations where fixing to Coulomb, Landau or Abelian gauge is required (see for example Refs. [52–54]). We perform 10000 sweeps of simulated annealing combined with overrelaxation. The divergence $\Delta(x)$ of the equivalent of the continuum gauge field, Eq. (A.8), computed through

$$\Delta(x) = \sum_i \left(A_i(x) - A_i(x-\hat{\imath})\right) \tag{A.11}$$

can be normed to give a measure θ of the quality of the gauge fixing,

$$\theta = \frac{1}{3V}\sum_x \mathrm{Tr}\,\Delta(x)\Delta^\dagger(x). \tag{A.12}$$

After our gauge fixing procedure we typically obtain $\theta \approx 10^{-11}$ given an initial value around 10^{-2}.

The above algorithm as implemented in our code is fully parallelised so the need to fix the gauge to produce meaningful particle number results is, overall, not a significant burden.

To obtain the electric field $E_i^a(x,t)$ note that the Coulomb gauge condition is time-independent. We therefore carry out the gauge fixing procedure – with the same $g(x)$ – on plaquettes at two sequential timesteps $U_i^g(x,t)$ and $U_i^g(x,t+\delta t)$ and use these to approximate the electric field $E_i(x,t)$ through

$$\exp\left[-i\frac{g}{2}E_i^a(x,t)\sigma^a\,\delta t\right] \approx U_i^g(x,t+\delta t)U_i^{g\dagger}(x,t). \tag{A.13}$$

Note that the gauge transformation $g(x)$, while time independent, does not necessarily bring configurations on any other timestep into Coulomb gauge, so our estimation of the gauge-fixed electric field could have $\mathrm{O}(\delta t)$ errors.

Having obtained lattice approximations to $E_i^a(x,t)$ and $A_i^a(x,t)$ we can compute Eqs. (3.2-3.3) and obtain particle numbers for the system at a given time from Eq. (3.4).

Note that, as demonstrated previously in Ref. [43], at large particle numbers the gauge fixing procedure does not substantially affect the final results. One could infer the same conclusions as we reach in this paper from the transverse 'particle number' obtained without gauge fixing; the discrepancy is around 10%.

A.2 Gauge fixing in U(1)

The same principle is applied here, except that a simple gradient flow procedure easily determines the transformation $A_i(x,t) \to A_i'(x,t) + \Lambda(x,t)$ that satisfies the condition $\partial_i A_i = 0$. The same gauge transformation Λ can then be applied to the following timestep to obtain $E_i(x,t)$ in a manner analogous to that given above.

A.2.1 Numerical tests

We confirmed that our backreaction times and other principal results were logarithmic in the initial energy density ξ. We also checked that the results did not depend on the timestep size or the lattice volume V (we tested 128^3 and 256^3, both of which capture the parametric resonance well). While we can test the large-volume and infrared robustness of our results, the system is conformal and there is no mass scale. Therefore we cannot take the continuum limit or draw any conclusions about physics once particle numbers in the UV start to grow after backreaction.

The simulations should always satisfy the Gauss law. The worst-case total Gauss law violation $\sum_x G(x)^2/V$ in the non-Abelian case was around 10^{-10}, and occurred around the time of backreaction.

References

[1] **ATLAS Collaboration** Collaboration, G. Aad *et. al.*, *Combined search for the Standard Model Higgs boson using up to 4.9 fb^{-1} of pp collision data at $\sqrt{s} = 7$ TeV with the ATLAS detector at the LHC*, *Phys.Lett.* **B710** (2012) 49–66 [1202.1408].

[2] **CMS Collaboration** Collaboration, S. Chatrchyan *et. al.*, *Combined results of searches for the standard model Higgs boson in pp collisions at $\sqrt{s} = 7$ TeV*, *Phys.Lett.* **B710** (2012) 26–48 [1202.1488].

[3] F. L. Bezrukov and M. Shaposhnikov, *The Standard Model Higgs boson as the inflaton*, *Phys.Lett.* **B659** (2008) 703–706 [0710.3755].

[4] F. Bezrukov, J. Rubio and M. Shaposhnikov, *Living beyond the edge: Higgs inflation and vacuum metastability*, 1412.3811.

[5] F. Bezrukov and M. Shaposhnikov, *Higgs inflation at the critical point*, *Phys.Lett.* **B734** (2014) 249–254 [1403.6078].

[6] Y. Hamada, H. Kawai, K.-y. Oda and S. C. Park, *Higgs Inflation is Still Alive after the Results from BICEP2*, *Phys.Rev.Lett.* **112** (2014), no. 24 241301 [1403.5043].

[7] J. Barbon and J. Espinosa, *On the Naturalness of Higgs Inflation*, *Phys.Rev.* **D79** (2009) 081302 [0903.0355].

[8] C. Burgess, H. M. Lee and M. Trott, *Comment on Higgs Inflation and Naturalness*, *JHEP* **1007** (2010) 007 [1002.2730].

[9] F. Bezrukov, A. Magnin, M. Shaposhnikov and S. Sibiryakov, *Higgs inflation: consistency and generalisations*, *JHEP* **1101** (2011) 016 [1008.5157].

[10] J. Espinosa, G. Giudice and A. Riotto, *Cosmological implications of the Higgs mass measurement*, *JCAP* **0805** (2008) 002 [0710.2484].

[11] A. De Simone and A. Riotto, *Cosmological Perturbations from the Standard Model Higgs*, *JCAP* **1302** (2013) 014 [1208.1344].

[12] K. Enqvist, T. Meriniemi and S. Nurmi, *Generation of the Higgs Condensate and Its Decay after Inflation*, *JCAP* **1310** (2013) 057 [1306.4511].

[13] K. Enqvist, T. Meriniemi and S. Nurmi, *Higgs Dynamics during Inflation*, *JCAP* **1407** (2014) 025 [1404.3699].

[14] A. Kobakhidze and A. Spencer-Smith, *Electroweak Vacuum (In)Stability in an Inflationary Universe*, *Phys.Lett.* **B722** (2013) 130–134 [1301.2846].

[15] M. Fairbairn and R. Hogan, *Electroweak Vacuum Stability in light of BICEP2*, *Phys.Rev.Lett.* **112** (2014) 201801 [1403.6786].

[16] A. Hook, J. Kearney, B. Shakya and K. M. Zurek, *Probable or Improbable Universe? Correlating Electroweak Vacuum Instability with the Scale of Inflation*, *JHEP* **1501** (2015) 061 [1404.5953].

[17] J. R. Espinosa, G. F. Giudice, E. Morgante, A. Riotto, L. Senatore *et. al.*, *The cosmological Higgstory of the vacuum instability*, 1505.04825.

[18] A. De Simone, H. Perrier and A. Riotto, *Non-Gaussianities from the Standard Model Higgs*, *JCAP* **1301** (2013) 037 [1210.6618].

[19] K.-Y. Choi and Q.-G. Huang, *Can the standard model Higgs boson seed the formation of structures in our Universe?*, *Phys.Rev.* **D87** (2013), no. 4 043501 [1209.2277].

[20] K. Enqvist, S. Nurmi, T. Tenkanen and K. Tuominen, *Standard Model with a real singlet scalar and inflation*, *JCAP* **1408** (2014) 035 [1407.0659].

[21] A. Kusenko, L. Pearce and L. Yang, *Postinflationary Higgs relaxation and the origin of matter-antimatter asymmetry*, *Phys.Rev.Lett.* **114** (2015), no. 6 061302 [1410.0722].

[22] F. Bezrukov, M. Y. Kalmykov, B. A. Kniehl and M. Shaposhnikov, *Higgs Boson Mass and New Physics*, *JHEP* **1210** (2012) 140 [1205.2893].

[23] G. Degrassi, S. Di Vita, J. Elias-Miro, J. R. Espinosa, G. F. Giudice *et. al.*, *Higgs mass and vacuum stability in the Standard Model at NNLO*, *JHEP* **1208** (2012) 098 [1205.6497].

[24] D. Buttazzo, G. Degrassi, P. P. Giardino, G. F. Giudice, F. Sala *et. al.*, *Investigating the near-criticality of the Higgs boson*, *JHEP* **1312** (2013) 089 [1307.3536].

[25] A. Kobakhidze and A. Spencer-Smith, *The Higgs vacuum is unstable*, 1404.4709.

[26] A. Spencer-Smith, *Higgs Vacuum Stability in a Mass-Dependent Renormalisation Scheme*, 1405.1975.

[27] M. Herranen, T. Markkanen, S. Nurmi and A. Rajantie, *Spacetime curvature and the Higgs stability during inflation*, *Phys.Rev.Lett.* **113** (2014), no. 21 211102 [1407.3141].

[28] **BICEP2** Collaboration, P. Ade *et. al.*, *Detection of B-Mode Polarization at Degree Angular Scales by BICEP2*, *Phys.Rev.Lett.* **112** (2014), no. 24 241101 [1403.3985].

[29] **Planck** Collaboration, P. Ade *et. al.*, *Planck 2015 results. XIII. Cosmological parameters*, 1502.01589.

[30] F. Bezrukov, D. Gorbunov and M. Shaposhnikov, *On initial conditions for the Hot Big Bang*, *JCAP* **0906** (2009) 029 [0812.3622].

[31] J. Garcia-Bellido, D. G. Figueroa and J. Rubio, *Preheating in the Standard Model with the Higgs-Inflaton coupled to gravity*, *Phys.Rev.* **D79** (2009) 063531 [0812.4624].

[32] K. Enqvist, S. Nurmi and S. Rusak, *Non-Abelian dynamics in the resonant decay of the Higgs after inflation*, *JCAP* **1410** (2014), no. 10 064 [1404.3631].

[33] D. G. Figueroa, J. Garcia-Bellido and F. Torrenti, *The Decay of the Standard Model Higgs after Inflation*, 1504.04600.

[34] A. Starobinsky, *Stochastic de sitter (inflationary) stage in the early universe*, in *Field Theory, Quantum Gravity and Strings* (H. Vega and N. Snchez, eds.), vol. 246 of *Lecture Notes in Physics*, pp. 107–126. Springer Berlin Heidelberg, 1986.

[35] A. A. Starobinsky and J. Yokoyama, *Equilibrium state of a selfinteracting scalar field in the De Sitter background*, *Phys.Rev.* **D50** (1994) 6357–6368 [astro-ph/9407016].

[36] K. Enqvist, R. N. Lerner, O. Taanila and A. Tranberg, *Spectator field dynamics in de Sitter and curvaton initial conditions*, *JCAP* **1210** (2012) 052 [1205.5446].

[37] J. H. Traschen and R. H. Brandenberger, *PARTICLE PRODUCTION DURING OUT-OF-EQUILIBRIUM PHASE TRANSITIONS*, *Phys.Rev.* **D42** (1990) 2491–2504.

[38] L. Kofman, A. D. Linde and A. A. Starobinsky, *Reheating after inflation*, *Phys. Rev. Lett.* **73** (1994) 3195–3198 [hep-th/9405187].

[39] L. Kofman, A. D. Linde and A. A. Starobinsky, *Towards the theory of reheating after inflation*, *Phys.Rev.* **D56** (1997) 3258–3295 [hep-ph/9704452].

[40] P. B. Greene, L. Kofman, A. D. Linde and A. A. Starobinsky, *Structure of resonance in preheating after inflation*, *Phys.Rev.* **D56** (1997) 6175–6192 [hep-ph/9705347].

[41] A. Rajantie, P. Saffin and E. J. Copeland, *Electroweak preheating on a lattice*, *Phys.Rev.* **D63** (2001) 123512 [hep-ph/0012097].

[42] A. Diaz-Gil, J. Garcia-Bellido, M. G. Perez and A. Gonzalez-Arroyo, *Primordial magnetic fields from preheating at the electroweak scale*, *JHEP* **0807** (2008) 043 [0805.4159].

[43] J.-I. Skullerud, J. Smit and A. Tranberg, *W and Higgs particle distributions during electroweak tachyonic preheating*, *JHEP* **0308** (2003) 045 [hep-ph/0307094].

[44] G. Aarts and J. Smit, *Particle production and effective thermalization in inhomogeneous mean field theory*, *Phys.Rev.* **D61** (2000) 025002 [hep-ph/9906538].

[45] M. Salle, J. Smit and J. C. Vink, *Thermalization in a Hartree ensemble approximation to quantum field dynamics*, *Phys.Rev.* **D64** (2001) 025016 [hep-ph/0012346].

[46] D. Bodeker and K. Rummukainen, *Non-abelian plasma instabilities for strong anisotropy*, *JHEP* **0707** (2007) 022 [0705.0180].

[47] R. Micha and I. I. Tkachev, *Relativistic turbulence: A Long way from preheating to equilibrium*, *Phys. Rev. Lett.* **90** (2003) 121301 [hep-ph/0210202].

[48] R. Micha and I. I. Tkachev, *Turbulent thermalization*, *Phys. Rev.* **D70** (2004) 043538 [hep-ph/0403101].

[49] J. Berges, K. Boguslavski, S. Schlichting and R. Venugopalan, *Turbulent thermalization process in heavy-ion collisions at ultrarelativistic energies*, *Phys. Rev.* **D89** (2014), no. 7 074011 [1303.5650].

[50] A. Kurkela and G. D. Moore, *Thermalization in Weakly Coupled Nonabelian Plasmas*, *JHEP* **12** (2011) 044 [1107.5050].

[51] S. Fachin and C. Parrinello, *Global gauge fixing in lattice gauge theories*, *Phys.Rev.* **D44** (1991) 2558–2564.

[52] L. Giusti, M. Paciello, C. Parrinello, S. Petrarca and B. Taglienti, *Problems on lattice gauge fixing*, *Int.J.Mod.Phys.* **A16** (2001) 3487–3534 [hep-lat/0104012].

[53] G. Bali, V. Bornyakov, M. Muller-Preussker and F. Pahl, *New algorithm for gauge fixing in SU(2) lattice gauge theory*, *Nucl.Phys.Proc.Suppl.* **42** (1995) 852–854 [hep-lat/9412027].

[54] M. Schröck and H. Vogt, *Coulomb, Landau and Maximally Abelian Gauge Fixing in Lattice QCD with Multi-GPUs*, *Comput.Phys.Commun.* **184** (2013) 1907–1919 [1212.5221].